Probing Metal Complexation, Structure, Ligand Lability and Dissociative Ligand-Exchange Mechanism in the Slipped Triple-Decker Complexes [{(η^5-Cp^R)Co}$_2$-μ-{η^4:η^4-arene}] (R = Me$_5$, 1,2,4-tri-*tert*-butyl; arene = toluene, benzene)

Jörg J. Schneider,* Dirk Wolf, Christoph Janiak, Oliver Heinemann, Jörg Rust, and Carl Krüger

Dedicated to Professor Peter Jutzi on the occasion of his 60th birthday

Abstract: Synthesis, structure, and reactivity of the slipped triple-decker complex [{(η^5-Cp^R)Co}$_2$-μ-{η^4:η^4-arene}] (**3**; R = 1,2,4-tri-*tert*-butyl) is described. A unique feature of the compound is its η^4:η^4 antifacial-coordinated arene ligand, which displays complete planarity, as determined by X-ray crystallography, and represents the first example of its kind. In **3** two opposite carbon atoms of the arene moiety are bonded to both cobalt centers. To probe possible reasons for arene lability in this complex we compared arene exchange with benzene and azulene in **3** and in the related complex [{(η^5-Cp^R)Co}$_2$-μ-{η^4:η^4-arene}] (**1**; R = Me$_5$). Compounds **1** and **3** react with azulene at room temperature displaying an unusual ligand exchange reactivity. The molecular structures of the reaction products of **3** with different azulenes, [{(η^5-Cp^R)Co}$_2$-μ-{η^4:η^4-azulene*}] (R = 1,2,4-tri-*tert*-butyl; azulene* = azulene **8**; 1,3,5-trimethylazulene **9**; 1,4 dimethyl-7-*iso*-propylazulene **10**), were determined by X-ray crystallography. These showed a *trans* arrangement of the Cp^R fragments on opposite sides of the five- and seven-membered rings of the bridging azulene ligand, with distinct coordination in the ligand periphery of the five- and seven-membered rings of the π system. Theoretical calculations on the model compound [{(η^5-Cp)Co}$_2$-μ-{η^4:η^4-arene}] **4** were performed with the semiempirical ZINDO approximation. From a crossover exchange experiment between **1**, **3**, benzene, and azulene it was deduced that arene exchange in these triple-deckers proceeds by a *dissociative* pathway involving mononuclear {(η^5-Cp^R)Co} intermediates (R = Me$_5$, 1,2,4-tri-*tert*-butyl). The formation of the mixed triple-decker **13** as main product in this experiment is highly indicative for this type of ligand substitution. Such a mechanism is described herein, for the first time, for ligand exchange in triple-decker complexes.

Keywords: arene complexes · arene exchange · azulene · cobalt · sandwich complexes

Introduction

The sequential formation, functionalization, and cleavage of arene transition metal π bonds is of paramount importance in stoichiometric as well as catalytic organometallic synthesis.[1] Arene exchange and change in hapticity processes in mononuclear, monocyclic arene complexes have been studied either thermally, photochemically, or by redox activation.[2] However, this is not so with dinuclear complexes containing bridging monocyclic arenes (e.g. substituted benzenes), simply due to a lack of compounds exhibiting this unique reactivity pattern. Triple-decker sandwich compounds in which six-membered arene rings are simultaneously and equivalently bonded to two metal atoms lying opposite to each other above and below the ring are especially rare.[3] Synthetic utility of this interesting type of complex in stoichiometric or even catalytic reactions should be warranted when the exchange process is possible at ambient temperature, thus allowing mild reaction conditions for an exchange. Recently we reported the first synthetic approach towards triple-decker compounds exhibiting this characteristic reactivity (Figure 1).[4] In type **1** complexes an alkyl-substituted arene (e.g., toluene, *o*-, *m*-, or *p*-xylene, or *iso*-propylbenzene)

[*] Priv.-Doz. Dr. J. J. Schneider, Dipl.-Chem. D. Wolf
Institut für Anorganische Chemie der Universität-GH Essen
Universitätsstrasse 5–7, D-45117 Essen (Germany)
Fax: (+49) 201-183-2402.
E-mail: joerg.schneider@uni-essen.de
Priv.-Doz. Dr. C. Janiak
Institut für Anorganische Chemie der Universität Freiburg
Albertstrasse 21, D-79104 Freiburg (Germany).
Dr. O. Heinemann, J. Rust, Prof. Dr. C. Krüger
Max-Planck-Institut für Kohlenforschung, Kaiser-Wilhelm-Platz 1
D-45470 Mülheim an der Ruhr (Germany).

  0947-6539/98/0410-1982 $ 17.50+.50/0

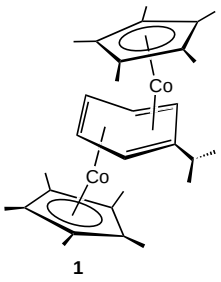

1

Figure 1. Structure of the slipped triple-decker **1** in the solid state.[4]

coordinates as the middle deck to two {Me_5CpCo} fragments in a hitherto unprecedented antifacial η^4:η^4 coordination mode in which the bridging arene has a puckered chairlike conformation (Figure 1).

The arene middle deck in **1** (R = Me_5) displays an unusual reaction chemistry in that the arene can be exchanged at room temperature for a variety of ligands (e.g., various other arenes, cycloheptatriene, cyclooctatetraene) under retention of the η^4:η^4 puckered coordination mode and the antifacial binuclear structure of the newly incoming arene, as well as the cyclic C7 and C8 π systems.[4, 5]

Inspired by the results of these studies the question about the mechanism of the ligand exchange in **1** arose, and an answer to it is of fundamental interest for a general understanding of exchange reactions of triple-decker complexes in organometallic chemistry.

Results and Discussion

Assuming that steric effects at the terminal Cp ligands should alter the geometry and/or coordination mode of the arene middle deck of **1**, we suspected that by separating the influence of these effects the origin of the high reactivity of **1** may be traceable. Therefore we introduced highly steric demanding 1,2,4-tri-*tert*-butyl-Cp ligands in the periphery of the triple-decker type complex **1** in order to probe differences in the structures of the bridging arene ligand in solution (by ^{1}H NMR) and in the solid state (by X-ray crystallography), in their arene exchange characteristics (versus azulene and benzene), and in their electronic structure (semiempirical ZINDO/S level).

Synthesis: Introducing bulky 1,2,4-tri-*tert*-butyl-Cp ligands instead of Me_5Cp groups in **1** should result in a distinct variation of steric effects in the triple-decker structure. Dehalogenation of the bridged dichloro or dibromo complex **2**[6] in a 100-fold excess of toluene with potassium metal results in the formation of deep red crystals of **3** in 50% yield (Scheme 1).

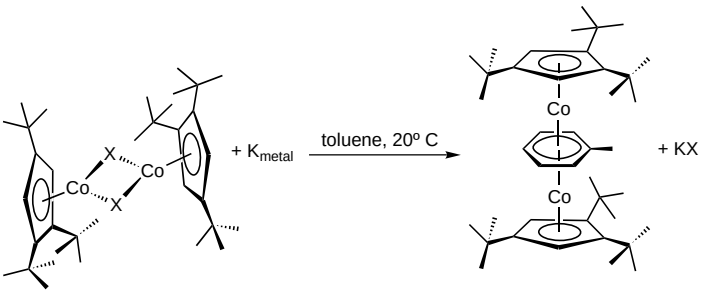

X = Cl, Br **2** **3**

Scheme 1. Formation of the triple-decker **3**.

Compound **3** is highly soluble in pentane, toluene, and ether and is air stable for short periods of time in the solid state; if stored under an inert atmosphere, it is stable for several months. In the EI mass spectrum, the [M^+] ion of **3** is observed confirming its dinuclear composition. The ^{1}H NMR spectrum of **3** in solution is in agreement with this result, showing an overall proton ratio of the 1,2,4-tri-*tert*-butyl-Cp:toluene of 2:1. The aromatic protons of the toluene ligand appear as three well-separated multiplets (t, d, t) between $\delta = 4.1$ and 3.8 according to the influence of the two coordinated {(η^5-Cp^R)Co} metal fragments on the arene, thus indicating a coordination that would be expected for a complex with a symmetrically μ-η^6:η^6 coordinated toluene ligand. Variation of the temperature between $-80\,^\circ$C and $+80\,^\circ$C does not effect the appearance of the spectrum, in agreement with a highly fluctional coordination mode of the two {(η^5-Cp^R)Co} fragments to the bridging toluene ligand in solution. With respect to these observations, **3** shows the same characteristics as the Me_5Cp derivative **1**.

The molecular structure of **3** in the solid state was determined by single-crystal X-ray analysis (Figure 2). The toluene ligand bridges the two 1,2,4-tri-*tert*-butyl-Cp complex fragments in an η^4:η^4 antifacial arrangement, which results in a slipped triple-decker structure. The atoms C13 and C16 of the toluene ligand are bonded to both Co atoms, and their bond lengths are therefore significantly elongated compared with the other Co–C_{ring} distances. With regard to this, the structure corresponds to that of triple-decker **1** (arene = *iso*-propylbenzene).[4] High thermal-anisotropic factors for the arene C atoms in **3**, also observed for **1**, point towards a dynamic and nonstatic behavior of the bridging arene ligand even in the solid state. For polycrystalline **1** we have already verified this by solid-state CP-MAS NMR spectroscopy.[4]

Abstract in German: *Synthese, Struktur und Reaktivität des Tripeldeckers [{(η^5-Cp^R)Co}$_2$-μ-{η^4:η^4-Aren}] (R = 1,2,4-tri-tert-Butyl; Aren = Toluol) mit verbrückendem π-Arenliganden werden beschrieben. Die Reaktivität von **3** und [{(η^5-Cp^R)Co}$_2$-μ-{η^4:η^4-Aren}] (R = Me_5, Aren = Toluol, Benzol) **1** wird im Hinblick auf den Aren-Ligandenaustausch untersucht, dabei wird eine hohe Reaktivität gegenüber verschiedenen Azulenen festgestellt. In den zweikernigen Azulenkomplexen besteht eine antarafaciale Koordination der [(η^5-Cp^R)Co] Metalligandeinheiten an den verbrückenden Azulenliganden. Die Koordination der Metalligandfragmente an den nicht benzenoiden Azulenliganden spiegelt die dipolare Grenzstruktur wider, mit einer Ladungslokalisation in der terminalen Ligandperipherie. Durch Kreuzungsexperimente zum Arenaustausch von **1** und **3** wird ein dissoziativer Ligandenaustauschmechanismus für diese Tripeldecker nachgewiesen. Dabei werden in Lösung aus **1** und **3** hochreaktive 20 e Sandwichkomplexe [(η^5-Cp^R)Co(η^6-Aren)] (R = Me_5, 1,2,4-tri-tert-Butyl; Aren = Benzol, Toluol) gebildet und 14 e [(η^5-Cp^R)] Ligandfragmente (R = Me_5, 1,2,4-tri-tert-butyl) auf diese in situ übertragen.*

  0947-6539/98/0410-1983 $ 17.50+.25/0

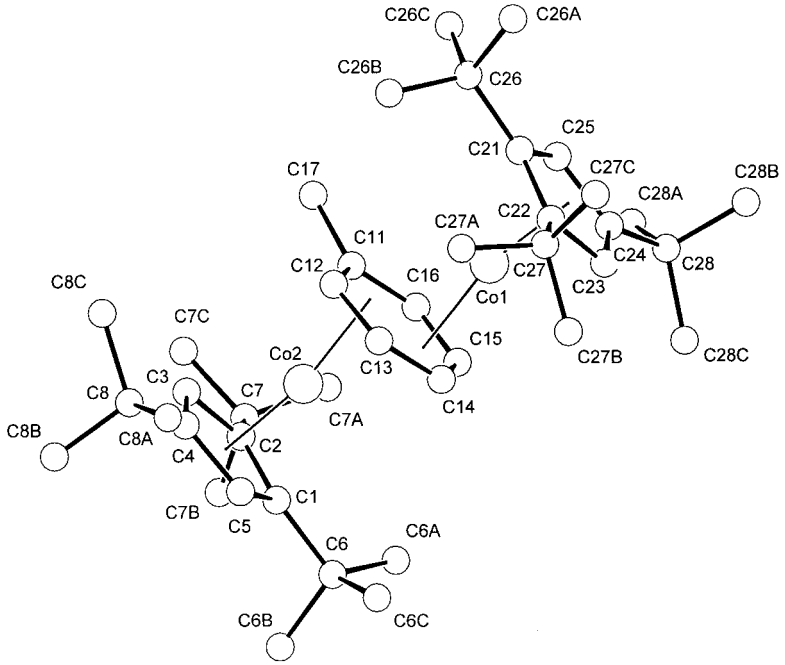

Figure 2. Molecular structure of **3** in the crystal. Selected bond lengths [Å]: Co1–C13 2.294(9), Co1–C15 2.10(1), Co1– C14 2.05(1), Co1–C16 2.394(8), Co2–C12 2.107(8), Co2–C16 2.33(1), Co2–C13 2.386(8), Co2–C11 2.092(8).

The relative orientation of the two {(η^5-Cp)Co} fragments with respect to each other reveals an important difference when comparing the solid-state structures of **1** and **3**. In **1** the two Co centers share two neighboring carbon atoms of the arene ring (Figure 3a), while in **3** two opposite carbon atoms of the arene moiety are bonded to both of the Co centers (Figure 3b). In the following the former bonding mode will be termed unsymmetrical η^4:η^4 and the latter symmetrical η^4:η^4.

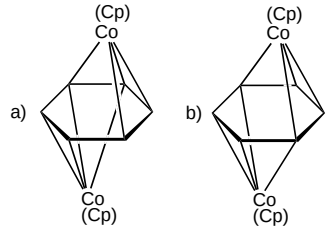

Figure 3. Schematic illustration of the different Co–arene bonding modes found in the triple-decker complexes **1** and **3**; a) the unsymmetrical η^4:η^4 interaction observed in **1** and b) the symmetrical η^4:η^4 Co–arene contacts encountered in **3**.

Calculations: Molecular modeling studies on the semiempirical ZINDO level[7] of the model complex [{(η^5-Cp)Co}$_2$-μ-{η^4:η^4-C_6H_6}] (**4**) were performed to see if the distortion of arene ring in **1**, compared with no distortion in compound **3**, could be traced to a possible electronic origin. Both geometries were first optimized by ZINDO/1 calculations, which in the unsymmetrical η^4:η^4 case produced a slightly distorted arene ring, whereas in the symmetrical η^4:η^4 interaction the arene ring remained planar. Molecular-orbital calculations by the ZINDO/S methodology were then performed on the ZINDO/1 optimized geometries in order to gain insight into the unusual η^4:η^4 arene type coordination to two {CpCo} fragments. As a consequence of the different modes of Co–arene bonding in **1** and **3**, the highest occupied molecular orbitals obtained from a semiempirical ZINDO/S calculation (Figure 4) differ somewhat in their composition and character. Both HOMOs are Cp–Co antibonding. The Co–arene interaction is more complicated: as anticipated, the interaction along the long Co–C distances is antibonding, and a weak bonding mode is present along two of the shorter Co–C contacts. In the symmetrical η^4:η^4 type (Figure 4b) this bonding to the inner two out of the four closer Co–C arene–carbon contacts might help to explain the observed variation in the Co–C arene bonds in **3**, namely, that the two inner Co–C distances are significantly shorter (by 0.2 to 0.3 Å) than the outer two Co–C bond distances. In the unsymmetrical η^4:η^4 mode (Figure 4a) one of the cobalt atoms dominates the arene interactions in the HOMO, while the other one is involved in the energetically well-separated HOMO-1 orbital (not shown here). In contrast to the symmetric-η^4:η^4 type, the two orbitals have a bonding interaction along the two outer Co–C bonds. This may be traced to an electronic origin of the arene-ring distortion.

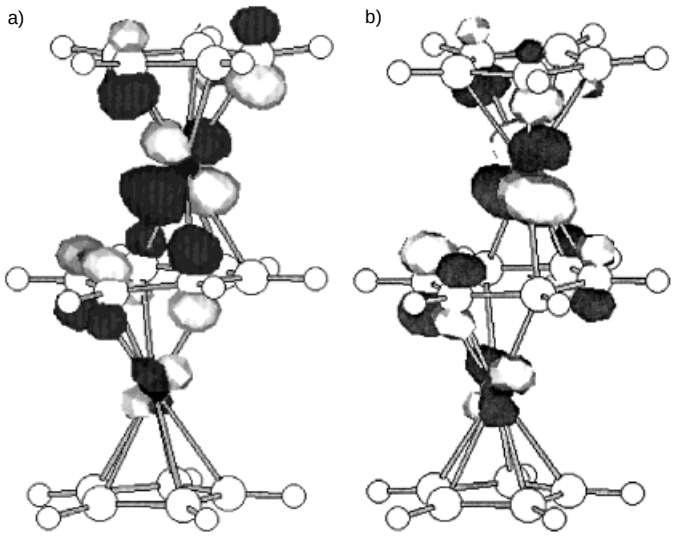

Figure 4. Highest occupied molecular orbitals of the metal complex [{(η^5-Cp)Co}$_2$-μ-{η^4:η^4-benzene}] (**4**) according to ZINDO/S calculations; a) unsymmetrical η^4:η^4, and b) symmetrical η^4:η^4 Co–arene interaction.

Exchange reaction of 1 and 3 with azulene: Recently we have reported on the high ligand lability of **1** towards a variety of different ligands, all of which are capable of displacing the bridging arene under very mild conditions.[4, 5] One result of these studies was that we could not observe any acceleration or slowing down of the exchange rate when ligand substitution on the incoming ligand molecule is varied.

In order to probe if the different structures for **1** and **3** have consequences for the structure–reactivity relationship, and to see whether the bulky tri-*tert*-butyl-Cp substitution in **3** has any significant effect on the arene-exchange reaction rate**,** we choose to carry out an arene- versus azulene-exchange

0947-6539/98/0410-1984 $ 17.50+.50/0 *Chem. Eur. J.* **1998**, *4*, No. 10

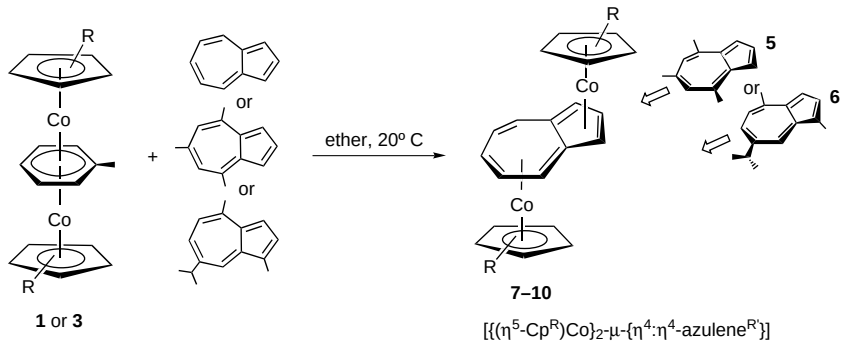

Scheme 2. Reaction of **1** and **3** with azulene. **1**: R = Me_5; **3**: R = 1,2,4-tri-*tert*-butyl; **7**: R = Me_5, R′ = H; **8**: R = 1,2,4-tri-*tert*-butyl, R′ = H; **9**: R = 1,2,4-tri-*tert*-butyl, R′ = 1,3,5-trimethyl; **10**: R = 1,2,4-tri-*tert*-butyl, R′ = 7-*iso*-propyl-2,4-dimethyl.

reaction of **1** and **3** at ambient temperature in ether (Scheme 2). Both triple-deckers react readily with one equivalent of azulene or the substituted azulenes **5** and **6** at 25 °C, under exchange of the arene middle deck against these nonbenzenoid ligands, to form the μ-azulene-bridged complexes [{(η^5-Cp^R)Co}$_2$-μ-{η^4:η^4-azulene$^{R'}$}] (R = Me_5, R′ = H **7**, R = 1,2,4-tri-*tert*-butyl, R′ = H **8**, R = 1,2,4-tri-*tert*-butyl, R′ = 1,3,5, trimethyl **9**, R = 1,2,4-tri-*tert*-butyl, R′ = 1,4-dimethyl, 7-*iso*-propyl **10**).

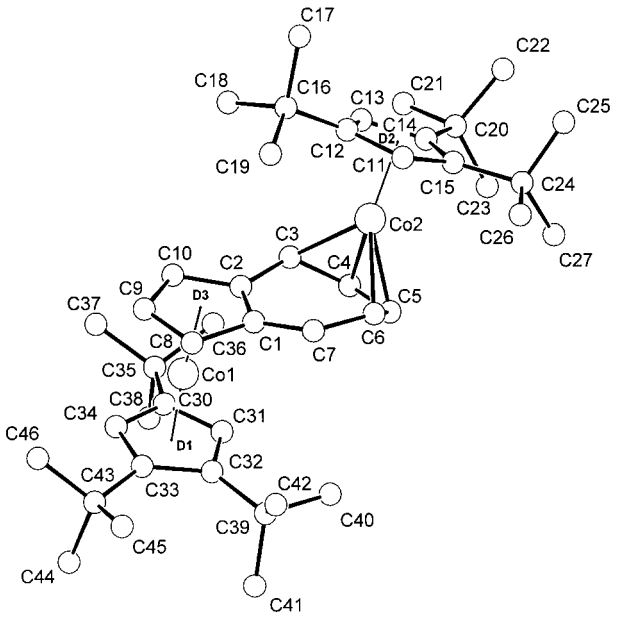

Figure 5. Molecular structure of **8** in the crystal. Selected bond lengths [Å]: Co1–C1 2.360(6), Co1–C2 2.156(6), Co1–C8 2.092(6), Co1–C9 1.984(7), Co2–C3 2.095(6), Co2– C4 1.968(6), Co2–C5 1.965(6), Co2–C6 2.167(7), C1–C2 1.478(8), C2–C10 1.437(8), C9–C10 1.42(1), C2–C3 1.474(8), C3–C4 1.411(9), C4–C5 1.427(9), C5–C6 1.37(1), C6–C7 1.473(9), C1–C7 1.355(9).

According to NMR and mass spectroscopic (MS) results, **7**–**10** all have dinuclear structures displaying a η^4:η^4 coordination of the two Co atoms to the bridging azulene moiety. Proof of the antifacial coordination of the two {(η^5-Cp^R)Co} fragments comes from X-ray crystal structures of **8**, **9**, and **10** (Figures 5, 6, and 7).

Each of the seven-membered rings of the azulene π system in **8**–**10** coordinates a {(1,2,4,tri-*tert*-butyl-η^5-Cp)Co} fragment in a η^4-bonding mode. The planes defined by the four cobalt-coordinated ring carbons of the seven-membered ring moieties of the azulene ligands are tilted by 37.4° (**8**), 33.5° (**9**), and 17.3° (**10**) against the planes through the uncoordinated carbon atoms of the seven-membered rings. Interestingly the five-membered rings of the azulenes are planar indicating a η^5 coordination of Co in contrast to the η^4 coordination mode observed in solution for **8**, **9**, and **10** by ^{1}H NMR, which might be an obvious contradiction at first sight. However, close inspection of the individual Co–C_{ring} bond lengths of the five-membered ring moieties reveal significantly elongated bond distances (Co1–C1, 2.306(6) Å **8**; Co1–C5, 2.411(3) Å, **9;** Co2–C22, 2.432(4) Å, **10**) when compared with the remaining four cobalt-to-carbon atom distances in these ring fragments of the azulene ligand; this indicates a distinct coordination shift $\eta^5 \rightarrow \eta^4$ clearly observable in the solid state. This effect is of course more profound in solution, resulting in a η^4:η^4-coordination of both {(η^5-1,2,4-tri-*tert*-butyl-Cp)Co} fragments to the bridging azulene ligands. An explanation for this behavior can be found in the dipolar nature of azulene (Figure 8), which manifests itself in a remarkable dipole moment of 0.8 D.[8]

Since the common-bridging bond of the five- and seven-membered ring of azulene has distinct single-bond character

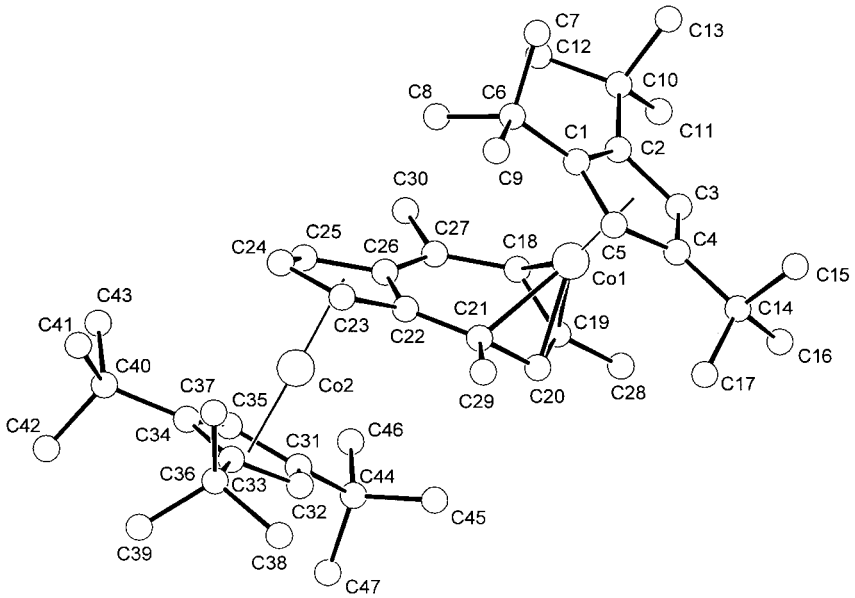

Figure 6. Molecular structure of **9** in the crystal. Selected bond lengths [Å]: Co1–C1 2.411(3), Co1–C2 2.075(3), Co1–C3 1.996(3), Co1–C3 1.996(3), Co1–C4 2.025(3), Co1–C5 2.170(3), Co2–C11 2.136(3), Co2–C12, 2.073(3), Co2–C13 2.099(3), Co2–C14 2.060(3), Co2–C15 2.141(3), C1–C5 1.474(4), C1–C2 1.453(4), C2–C3 1.428(5), C3–C4 1.420(5), C4–C5 1.447(5), C1–C10 1.445(4), C9–C10 1.417(5), C8–C9 1.434(5), C7–C8 1.472(5), C6–C7 1.343(5), C5–C6 1.432(5).

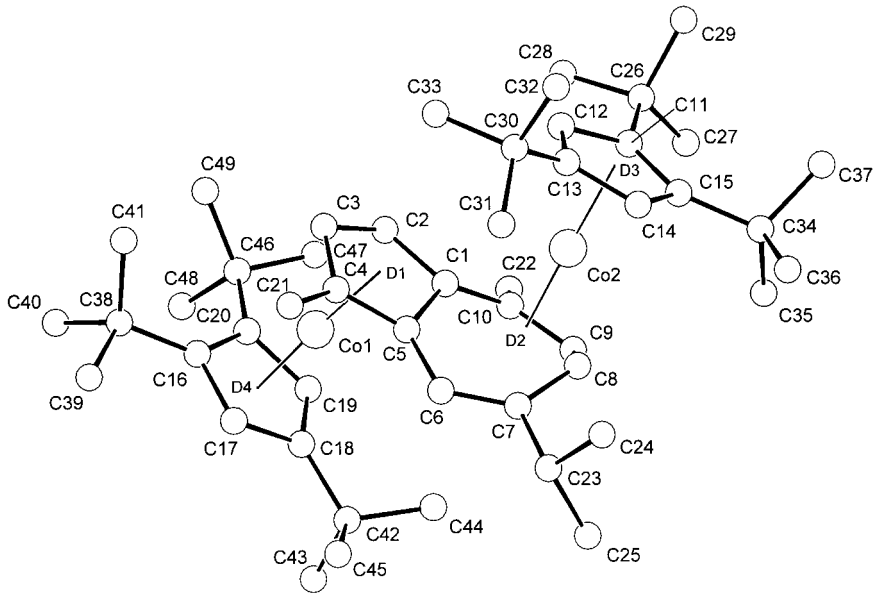

Figure 7. Molecular structure of **10** in the crystal. Selected bond lengths [Å]: Co2–C22 2.211(4), Co2–C23 2.0104(4), Co2–C24 1.990(5), Co2–C25 2.070(5), Co2–C26 2.432(4), Co1–C18 2.186(4), Co1–C19 1.971(4), Co1–C20 1.980(4), Co1–C21 2.189(5), C21–C22 1.439(6), C20–C21 1.447(7), C22–C26 1.484(6), C19–C20 1.398(6), C18–C19 1.430(6), C18–C27 1.460(6).

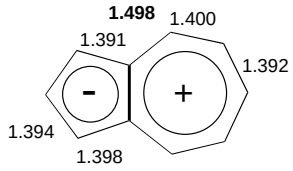

Figure 8. Dipolar resonance structure of azulene and bond lengths as determined by X-ray crystallography.[9]

(1.498 Å[9]), π conjugation within the π perimeter should be mainly in the periphery of the two ring systems, resulting in a shift of coordinated metal–ligand fragments to the outer carbon atoms of the five- and seven-membered rings. This is indeed observed in all three crystal structures (see Figure 9), indicating that this unusual coordination behavior is typical for this ligand type and reflects its dipolar nature.

For **1** and **3** all exchange reactions are completed within 30 minutes as can be seen by an intense color change from red-brown to purple. There is no indication of a significant slowing down in ligand exchange, neither by introducing the bulky 1,2,4-tri-*tert*-butyl-Cp ligand nor by introducing additional alkyl substituents on the bridging azulene perimeter. However, this fact is understandable when recalling that **1** and **3** show highly fluctional behavior in solution (by NMR, $T = 20\,^{\circ}C$ to $-80\,^{\circ}C$) indicating that energy barriers associated with the rotation of the bridging arene rings in these slipped triple-deckers are very small, thus equilibrating the different molecular structures for **1** and **3** in solution and, as a consequence, leading to no significant difference in ligand-exchange reactivity. However, this still leaves us with the question of the origin of the high ligand lability of **1** and **3**.

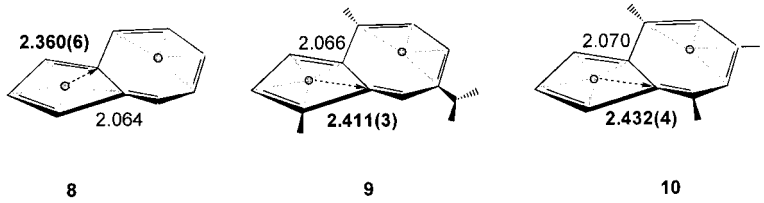

Figure 9. Schematic presentation of the metal coordination in the cobalt–azulene complexes **8**–**10** showing ring-slippage coordination of the {(1,2,4-tri-*tert*-butyl-Cp)Co} fragments towards the azulene-ligand periphery. All bond lengths are in Å. Plain numbers given are average values of the four remaining cobalt to carbon ring atom distances of the five-membered rings of the azulene ligands.

Competitive inter-arene-exchange experiments between 1 and 3:

An answer to the question of the origin of the unusual high arene-exchange activity for **1** and **3** must lie in the type of ligand-exchange mechanism operating for **1** and **3**. We set out to answer this question by conducting an arene-cross-over-exchange experiment (Scheme 3).

Two triple-deckers **A** and **B**, with different substitution patterns at their terminal ligands exchange a) their terminal metal–ligand fragments and b) their arene middle decks against a second arene ligand. In summary these two processes may result in formation of the mixed triple-decker **C** as main product if a dissociation prior to ligand exchange is operating. The arene exchange can be performed either on the mononuclear intermediates formed after the dissociation, or it may occur prior to dissociation of the metal–ligand fragments on the individual triple-decker complexes **A** and **B**. However, even in the latter case, formation of product **C** by a dissociative mechanism must be the crucial step and must be solely responsible for formation of the mixed complex **C**. No reasonable associative mechanism that does not involve a dissociation step of M–L fragments is able to explain formation of product **C** if it is formed.

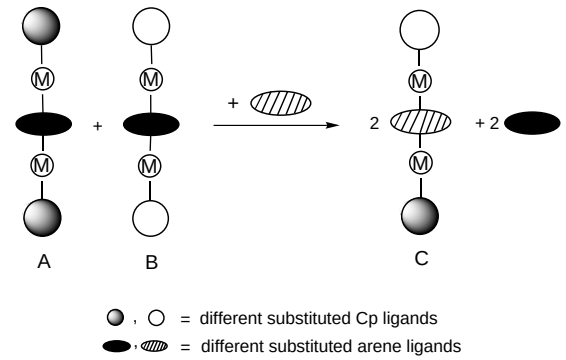

Scheme 3. Schematic outline of an dissociative ligand exchange in homo ligand triple-decker complexes **A** and **B** leading to a mixed hetero-ligand triple-decker complex **C**.

Mixing equimolar amounts of **1** and **3** in an excess of benzene (0.02 molar) and standing for 12 hours, followed by workup and crystallization from pen-

0947-6539/98/0410-1986 $ 17.50+.50/0 *Chem. Eur. J.* **1998**, *4*, No. 10

tane results in formation of the new triple-deckers **11** and **13** in a 1:6 ratio in 60% yield as brown crystals (Scheme 4). No attempts were made to separate this mixture of crystals any further.

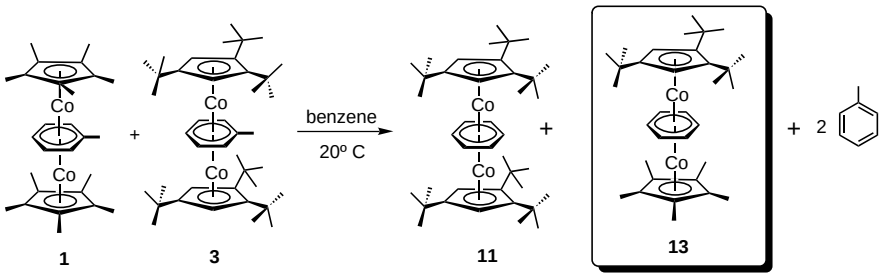

Scheme 4. Crossover arene-exchange experiment between **1**, **3** and excess benzene (0.02 molar concentration).

According to ^{1}H NMR analysis of this solid crystalline reaction material no formation of the bis-homo complex [{(η^5-Me_5Cp)Co}$_2$-μ-{η^4:η^4-benzene}] (**12**) was observed. The MS analysis of the isolated material confirmed the NMR results, showing distinct molecular ions of **11** and **13** together with corresponding characteristic fragment ions that can be assigned to these complexes. To ensure that no partial enrichment of **11** or **13** had occurred over any other component remaining in the solution during work up and crystallization, the mother liquor from which **11** and **13** were obtained was checked by NMR spectroscopy. This showed exactly the same ratio of **11** to **13** as in the already crystallized material**,** and there was no sign to indicate any formation of **12**. Therefore a significant formation of **12** can be excluded, since it must be below reasonable NMR detection limits (<100 μg).

The result of the benzene-exchange experiment is meaningful with respect to a more general understanding of ligand exchange in slipped triple-deckers **1** and **3**. The predominant formation of the mixed complex **13** (which corresponds to product **C** in Scheme 3) as the main product of the benzene exchange is most striking and strongly supports a dissociative mechanism of ligand exchange between **1**, **3**, and benzene as the substitution pathway. Highly reactive [(η^5-Cp^R)Co] (R = Me_5, 1,2,4,tri-*tert*-butyl) fragments must be transferred during the dissociation process. As a consequence, it is reasonable to assume that such a dissociative exchange accounts for the high ligand lability of **1** and **3** already reported earlier.[4, 5]

Which arguments—in addition to the above mentioned—also favor a dissociative exchange mechanism? There are two characteristic criteria that undoubtedly indicate a dissociative mechanism in ligand-substitution reactions. A dissociative mechanism should involve a reaction intermediate with lower coordination number, and the substitution rate of the exchange should be dependent on the off-coming ligand according to the general theory of Langford and Gray.[10, 11] The theory states that for a general ligand-substitution reaction [Equation (1)] where X is the leaving group, Y is the entering ligand, and L is the nonparticipating ligand(s), there are three general pathways: i) the dissociative (D)

$$ML_nX + Y \longrightarrow ML_nY + X \quad (1)$$

process, with an intermediate of lower coordination number, ii) the associative (A) process, with an intermediate of higher coordination number, and iii) the interchange (I) process, in which no intermediate of lower or higher coordination number is involved.

The latter possibility is further subdivided into two types: associative interchange (I_s) or dissociative interchange (I_d). A schematic presentation of these mechanisms is given in Scheme 5.[12]

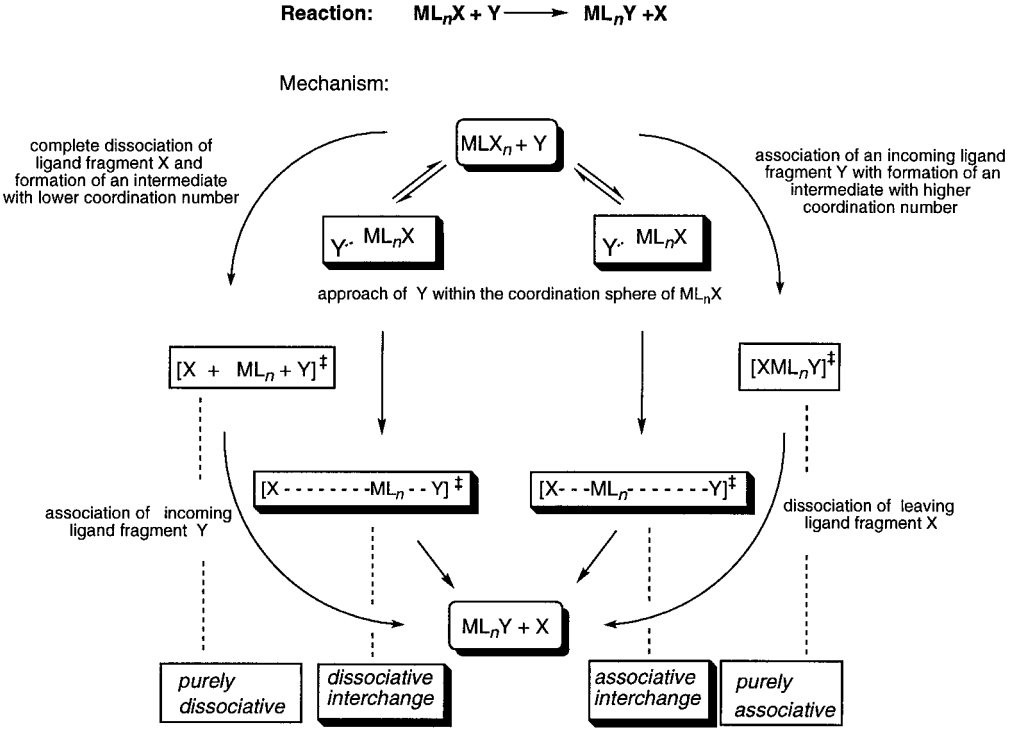

Scheme 5. Schematic representation of possible ligand-substitution mechanisms (adopted from ref. [12]).

In our earlier studies[4, 5] we have found that regardless of the type of newly incoming ligand, we observed no marked differences in the exchange reactivity when changing the incoming ligand, particularly on changing its electronic or steric properties. All reactions went to completion within a reasonably short time with high yields, independent of the ligands used. Steric reasons also argue strongly against an associative arene-exchange mechanism for **1** and **3**. When mixing equimolar amounts of **1** and **3** in a noncoordinating solvent like cyclohexane[D_8] we observed no intermolecular arene-ligand exchange between these triple deckers. These results indicate that prior to exchange, a dissociation of the triple-deckers **1** and **3** in a coordinating solvent (e.g. ether, arene, etc.) with liberation of [(η^5-Cp^R)Co] fragments seems necessary to initiate the ligand exchange.

To test this hypothesis we followed arene exchange of toluene versus [D_6]benzene by ^{1}H NMR spectroscopy for **1** and **3**, with formation of the [D_6]benzene bridged triple-deckers **14** and **15** as final products (Scheme 6), and detected the formation of mononuclear paramagnetic heteroleptic mixed [(η^5-Cp^R)(η^6-arene)Co] (arene = [D_6]benzene, toluene) sandwich complexes **16** and **17**.

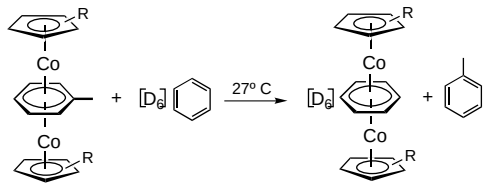

R = Me_5 **1**, R = 1,2,4-tri-*tert*-butyl **3** R = Me_5 **14**, R = 1,2,4-tri-*tert*-butyl **15**

Scheme 6. Arene exchange between **1** and benzene[D_6] leading to **14**.

Paramagnetic NMR shifts, are highly diagnostic for this class of Co sandwich compounds, rendering their identification unambiguous (Figure 10).[5] Nevertheless, to the best of our knowledge only two examples of this type of sandwich complexes are known so far.[5, 13]

For **3** similar results are observed for the toluene versus [D_6]benzene exchange; however, formation of the corresponding 1,2,4-tri-*tert*-butyl-substituted mixed heteroleptic sandwich complexes **18** and **19** is significantly slowed down compared with formation of **16** and **17**. Formation of the mixed sandwich complexes **16** and **18** can only be explained if dissociation of the triple-deckers **1** and **3** occurred prior to ligand exchange. This dissociation step must necessarily involve liberation of electronically unsaturated 14 e [(η^5-Cp^R)Co] fragments from the triple-deckers **1** and **3** (Scheme 7). These highly reactive metal–ligand fragments are unstable and are intercepted by reaction with excess [D_6]benzene and form triple-deckers [D_6]**1** and [D_6]**3**, and the mononuclear mixed sandwich complexes [D_6]**16** and [D_6]**18**.

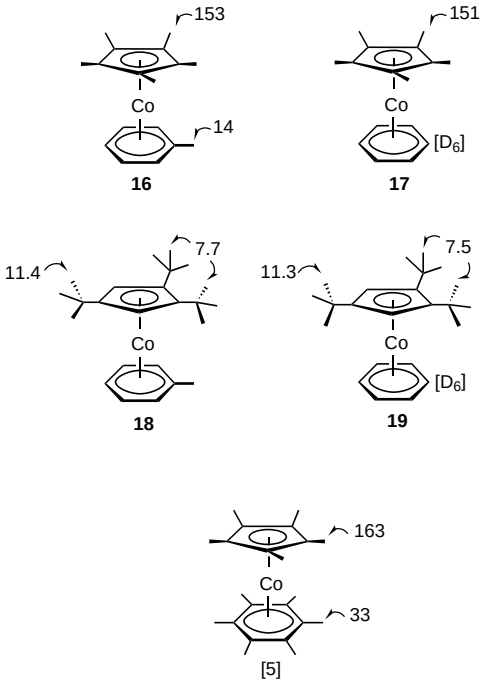

Figure 10. Mixed heteroleptic sandwich complexes **16**–**19** and paramagnetic ^{1}H NMR chemical shifts (relative to Tris) of their Cp^R ligands.

In situ synthesis of the heteroleptic sandwich complexes **16** and **18**, formed by degradation of the starting triple-deckers **1** and **3**, can also be observed by following the characteristic decrease of the ^{1}H NMR signals of the Cp^R ligands of triple-deckers **1** and **3** against time during the course of the exchange reaction (Figure 11). The decrease in intensity of the ^{1}H signal is accompanied by the parallel build up of intensity of the ^{1}H

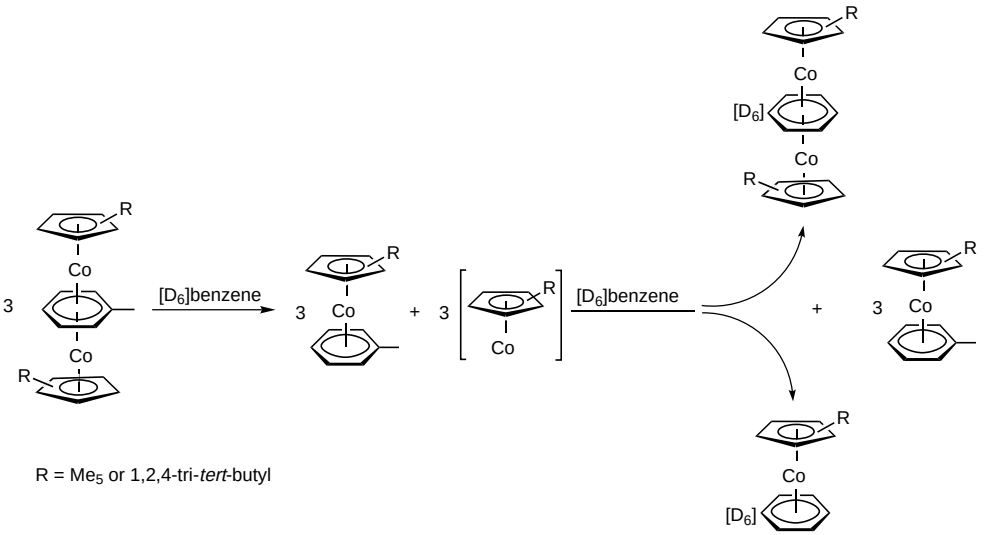

R = Me_5 or 1,2,4-tri-*tert*-butyl

Scheme 7. Dissociative degradation pathway of triple-deckers **1** and **3** with formation of mixed [(Cp)Co(arene)] sandwich complexes and liberation of 14 e {(Cp)Co} fragments.

0947-6539/98/0410-1988 $ 17.50+.50/0 *Chem. Eur. J.* **1998**, *4*, No. 10

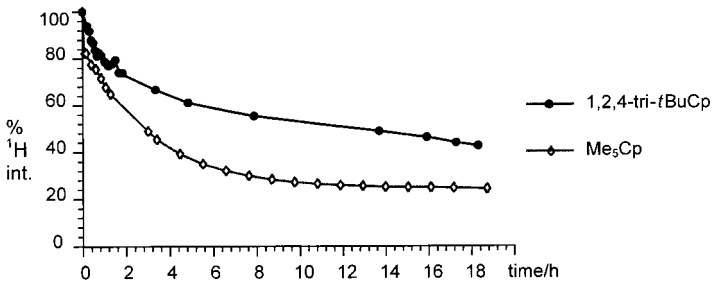

Figure 11. Decrease of ^{1}H NMR signal intensity of Me_5Cp and 1,2,4-tri-*tert*-butyl-Cp ligands of **1** and **3** versus reaction time. Proton intensity axis in arbitrary units.

signal of the Cp^R ligands of the newly formed heteroleptic sandwich complexes **16** and **18**, which are formed by dissociative degradation of the triple-deckers **1** and **3**. For the 1,2,4,tri-*tert*-butyl-Cp-substituted triple-decker **3**, the decrease in the intensity of the ^{1}H NMR signal with time is again significantly much less pronounced than for the Me_5Cp case **1**, as Figure 11 proves; this points towards a reduced arene-exchange reactivity of **3** compared with **1**.

In summary, the NMR results probe a) a dissociation of 14 e $[(\eta^5\text{-}Cp^R)Co]$ fragments from triple-deckers **1** and **3** and b) a distinct dependence of the arene exchange on the nature of the off-coming $[(\eta^5\text{-}Cp^R)Co]$-ligand fragments, which is indicative of a dissociative mechanism. We are currently investigating the role of sandwich complexes **16–19** in the formation of the corresponding triple-deckers in detail and will report on our findings in a forthcoming paper.[14]

Competitive inter-arene/azulene-exchange experiments between 1 and 3: Mixing equimolar amounts of **1**, **3**, and azulene in ether and stirring for 12 hours, followed by workup and crystallization from ether/acetonitrile, results in the formation of a crystalline compound mixture containing the homo and the mixed $[\{(\eta^5\text{-}Cp^{R,R^*})Co\}_2\text{-}\mu\text{-}\{\eta^4\text{:}\eta^4\text{-azulene}\}]$ ($R = Me_5$, $R^* = 1,2,4\text{-tri-}tert\text{-butyl}$) complexes **7**, **8**, and **20a,b** (Scheme 8), as determined by ^{1}H and mass spectroscopy.

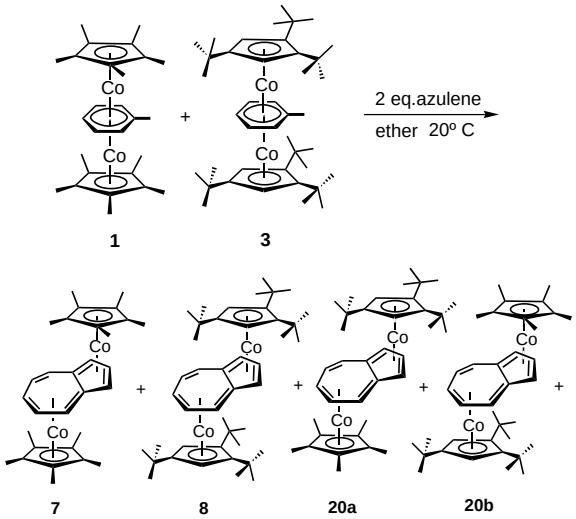

Scheme 8. Crossover arene-exchange experiment (equimolar concentrations) between **1**, **3** and azulene leading to **7**, **8** and **20a,b**.

For the mixed $[\{(\eta^5\text{-}Cp^{R,R^*})Co\}_2\text{-}\mu\text{-}\{\eta^4\text{:}\eta^4\text{-azulene}\}]$ ($R = Me_5$, $R^* = 1,2,4\text{-tri-}tert\text{-butyl}$) complexes **20a,b**, coordination of both $\{(Cp^{R,R^*})Co\}$ fragments either to the five- or seven-membered ring of the azulene π system is observed by ^{1}H NMR spectroscopy, giving rise to the formation of the two regio isomers **20a** and **20b**. On the basis of the ^{1}H NMR results we determined a 1:2 ratio of both regio isomers **20a**:**20b** and an overall ratio **7**:**8**:**20a,b** as 2:13:1 in the crystallized reaction product. As in the benzene exchange experiment, formation of the mixed azulene complexes **20a,b** is best explained by operation of a dissociative mechanism that is initiated by a ligand dissociation of the triple-deckers **1** and **3**. A sterically highly encumbered situation will be created if an alternative associative mechanism is assumed for the exchange reaction of **1** and **3** with azulene leading to **20a,b**. However, in view of products formed (**20a,b**), such a mechanism seems highly unlikely, if not impossible.

Conclusions

A new member of the rare class of triple deckers containing bridging arene ligands (**3**) was synthesized and structurally characterized in solution and in the solid state. Arene/azulene exchange reactions of triple-decker complexes **1** and **3** allow access to binuclear Co–azulene complexes **7–10**, which show a unique and different coordination mode in the solid state compared with the structure found in solution.

A remarkable result of our investigations towards probing a mechanism for ligand exchange in triple-deckers **1** and **3** lies in the fact that we were able to show that ligand exchange in the slipped triple-decker type complexes **1** and **3** proceeds by a dissociative pathway in which highly reactive 14 e $[(\eta^5\text{-}Cp^R)Co]$ fragments and mixed heteroleptic $[(\eta^5\text{-}Cp^R)Co(\eta^6\text{-arene})]$ sandwich-type complexes are formed. Examples for dissociative ligand-exchange processes are documented for mononuclear half-sandwich complexes.[2, 14] To the best of our knowledge, for related binuclear triple-decker sandwich complexes, such an exchange mechanism is described here for the first time.

Experimental Section

General considerations: All reactions were carried out under an atmosphere of dry nitrogen gas with standard Schlenk techniques. Microanalysis were performed by the microanalytical laboratory of the Chemistry Department of the University/GH Essen. Compounds **1** and **2** were prepared as reported,[4, 6] except that synthesis of **1** was carried out at $-20\,^\circ C$. All solvents were dried appropriately and were stored under nitrogen. Azulenes were commercial grade quality and were used without further purification. The NMR spectra were recorded on Bruker AC200, AC300, and WH400 spectrometers and referenced against the remaining protons of the deuterated solvent. NMR samples were prepared by vacuum transfer of solvents onto the appropriate amount of solid sample, followed by flame sealing of the NMR tube. MS spectra were recorded on a MAT8200 instrument with standard conditions (EI, 70 eV) and the fractional sublimation technique for compound inlet.

[{(1,2,4-tri-*tert*-butyl-η^5-Cp)Co}$_2$-μ-{η^4:η^4-toluene}] (**3**): $[\{(\eta^5\text{-}1,2,4\text{-tri-}tert\text{-butyl-Cp})CoX\}_2]$ ($X = Cl$ or Br)[6] (10 g, 15.3 mmol) was dissolved in toluene (150 mL), and potassium metal (16 mmol) was added in small pieces. The solution was then stirred for two weeks until all potassium

metal had dissolved. Removal of all volatiles under vacuum left an oily residue that was extracted with ether, filtered, concentrated, and cooled to −30 °C. After 24 h deep red crystals had separated in 40% yield. From the mother liquor a second crop of crystals could be obtained by prolonged cooling to −30 °C. MS (EI, 70 eV, T_{vap} 130 °C): *m/z* (%): 676 (80) [M^+], 384(72) [M^+ − (1,2,4-tri-*tert*-butyl-Cp)], 91(25), 57(100); ^{1}H NMR ([D$_8$]THF, 400 MHz, 27 °C): $\delta = 4.22$ (s, 4H), 4.10 (t, $J_{H,H} = 5.6$ Hz, 2H), 3.92 (d, $J_{H,H} = 5.0$ Hz, 2H), 3.80 (t, $J_{H,H} = 5.5$ Hz, 1H), 1.84 (s, CH_3), 1.40 (s, 36H), 1.21 (s, 18H); ^{13}C{^{1}H} NMR ([D$_8$]THF, 100.1 MHz, 27 °C): $\delta = 103.0$, 101.6, 72.50, 67.8, 59.80, 55.0, 54.0, 34.80, 33.0, 32.2, 31.2, 24.30; $C_{41}H_{29}Co_2$ (676.84): calcd C 72.76, H 9.83; found C 72.70, H 10.01.

[{(η^5-Cp^R)Co}$_2$-μ-{η^4:η^4-azulene^R}] (7; R = Me$_5$, R′ = H), (8; R = 1,2,4-tri-*tert*-butyl, R′ = H), (9; R = 1,2,4-tri-*tert*-butyl, R′ = 1,3,5, trimethyl), and (10; R = 1,2,4-tri-*tert*-butyl, R′ = 1,4-dimethyl, 7-*iso*-propyl): Compound **1** (**3**) (1 mmol) was dissolved in ether and the appropriate azulene (1.1 mmol) was added. After 30 minutes of stirring the color had changed from red-brown to purple. Stirring was continued for 12 hours, whereupon no additional changes occurred. Removal of all volatiles in vacuum, dissolution of the solid residue in ether/acetonitrile (5:2), and cooling to 0 °C for 12 hours resulted in the formation of black crystals of compounds **7**–**10** in 70–80% yield.

Compound **7**: MS (EI, 70 eV, T_{vap} 160 °C): *m/z* (%): 516 (100) [M^+], 329 (14) [(Me$_5$Cp)$_2$Co)], 322(9) [(Me$_5$Cp)(azulene)Co], 128(3) [azulene]; ^{1}H NMR ([D$_6$]benzene, 300 MHz, 27 °C): $\delta = 4.09$ (dd, $J_{H,H} = 7.8$ Hz, $J_{H,H} = 6.2$ Hz, 2H), 3.84 (d, $J_{H,H} = 2.3$ Hz, 2H), 3.62 (t, $J_{H,H} = 2.4$ Hz, 1H), 3.68 (t, $J_{H,H} = 6.2$ Hz, 1H), 3.52 (d, $J_{H,H} = 7.7$ Hz, 2H), 1.78 (s, 15H), 1.61 (s, 15H); ^{13}C{^{1}H} NMR ([D$_6$]benzene, 75.1 MHz, 27 °C): $\delta = 87.8$, 87.9, 77.9, 76.0, 68.4 (v br, $\tilde{\nu}_{1/2} = 25$ Hz), 71.6, 69.6, 10.3, 10.0; $C_{30}H_{38}Co_2$ (516.46): calcd C 69.76, H 7.42; found C 70.1, H 7.44.

Compound **8**: MS (EI, 70 eV, $T_{vap} = 100$ °C): *m/z* (%): 712(100) [M^+], 420(95) [M^+ − {(1,2,4-tri-*tert*-butyl-Cp)Co}], 57(60); ^{1}H NMR ([D$_8$]toluene, 200 MHz, 70 °C): $\delta = 4.69$ (dd, $J_{H,H} = 5.1$, 7.3 Hz, 2H), 4.51 (t, $J_{H,H} = 5.4$ Hz, 1H), 4.50 (d, $J_{H,H} = 2.5$ Hz, 2H), 4.50 (s, 2H), 4.34 (s, 2H), 3.94 (t, $J_{H,H} = 2.6$ Hz, 1H), 3.88 (d, $J_{H,H}$ 3.9 Hz, 2H), 1.29 (s, 18H), 1.28 (s, 18H), 1.19 (s, 9H), 1.14 (s, 9H); ^{13}C{^{1}H} NMR ([D$_8$]toluene, 100.1 MHz, 27 °C): $\delta =$ 106.46, 105.73, 103.78, 103.42, 78.2, 78.1, 76.2, 73.8, 69.31, 68.56, 34.6, 34.5, 33.6, 33.5, 32.2, 32.0, 31.89, 31.87.

Compound **9**: MS (EI, 70 eV, $T_{vap} = 120$ °C): *m/z* (%): 754(100) [M^+], 697 (22) [M^+ − *tert*-butyl], 461(17) [M^+ − {(1,2,4-tri-*tert*-butyl-Cp)Co}]; ^{1}H NMR ([D$_6$]benzene 27 °C , 300 MHz, 70 °C): $\delta = 1.25$ (s, 9H), 1,26 (s, 9H), 1.36 (s, 18H), 1.42 (s, 18H), 1.97 (s, 6H), 2.11 (s, 3H), 4.05 (s, 2H), 4.20 (t, $^3J_{H,H} = 2.64$, 1H), 4.37 (s, 2H), 4.39 (s, 2H), 4.67 (t, $^3J_{H,H} = 2.64$, 2H); ^{13}C{^{1}H} NMR ([D$_6$]benzene, 75.1 MHz, 27 °C) $\delta = 24.93$, 25.10, 31.03, 31.14, 31.29, 32.23, 32.74, 33.10, 33.27, 33.55, 33.87, 65.47, 66.62, 73.35, 75.37, 77. 96, 86. 14, 102. 81, 103. 58, 105. 82, 106. 21, 106, 11; $C_{47}H_{72}Co_2$ (754.91): calcd C 75.16, H 9.78; found C 75.14, H 9.92.

Compound **10**: MS (EI, 70 eV, $T_{vap} = 150$ °C): *m/z* (%): 782 (100) [M^+], 725(15), 489(17) [M^+ − {(1,2,4-tri-*tert*-butyl-Cp)Co}]; ^{1}H NMR ([D$_6$]benzene, 300 MHz, 27 °C): $\delta = 1.21$ (s, 9H), 1.25 (s, 9H), 1.27 (s, 9H), 1.32 (d, $^3J_{H,H} = 7.1$ Hz, 3H), 1.33 (s, 9H), 1.36 (s, 9H), 1.37 (d, $^3J_{H,H} = 7.1$, 3H), 1.49 (s, 9H), 2.06 (s, 3H), 2.61 (s, 3H), 2.63 (m, $^3J = 7.1$ Hz, 1H), 3.16 (d, $^3J_{H,H} =$ 7.3 Hz, 1H), 4.07 (d, $^3J_{H,H} = 2.38$ Hz, 1H), 4.12 (d, $^3J_{H,H} = 2.38$ Hz, 1H), 4.30 (d, $^3J_{H,H} = 7.3$ Hz, 1H), 4.47 (d, $^3J_{H,H} = 2.40$ Hz, 1H), 4.69 (d, $^3J_{H,H} = 7.3$ Hz, 1H), 4.89 (d, $^3J_{H,H} = 2.74$ Hz, 1H), 4.91 (s, 1H), 5.17 (d, $^3J_{H,H} = 2.38$ Hz, 1H); ^{13}C{^{1}H} NMR ([D$_6$]benzene, 75.1 MHz, 27 °C): $\delta = 15.56$, 22.58, 23.51, 24.68, 30.88, 31.56, 31.71, 32.21, 32.57, 32. 84, 32.86, 33.18, 33.78, 33.87, 34.18, 34.26, 38.10, 63.99, 74.17, 74.96, 75.05, 76.74, 76.83, 77.80, 86.13, 88.47, 100.92, 100.99, 101.93, 103.27, 103.84, 108.97; $C_{49}H_{76}Co_2$ (782.96): calcd C 74.78, H 9.61; found C 75.33, H 9.54.

Crossover exchange experiment between 1 and 3, and benzene: Compounds **3** and **1** (0.4 mmol) were dissolved in benzene (20 mL) resulting in a 0.02 molar solution. After standing for 12 hours at room temperature all volatiles were pumped off and the semicrystalline residue was dissolved in pentane, filtered, concentrated, and cooled to −78 °C giving a mixture of brown microcrystals (60 mg) of **11** and **13** in a 1:6 ratio according to ^{1}H NMR analysis. Ms of this mixture: EI (70 eV, $T_{vap} = 110$ °C): *m/z* (%): 662 (100) [M^+, **13**$^+$], 564 (18) [M^+, **11**$^+$], 370 (70) [**13**$^+$ − 1,2,4-tri-*tert*-butyl-Cp)], 272 (18) [**11**$^+$ − 1,2,4-tri-*tert*-butyl-Cp], 137 (6) [$C_6H_6Co^+$], 78 (27) [$C_6H_6^+$]; ^{1}H NMR analysis of the mixture: **11**: 1.28 (s, 9H), 1.50 (s, 18H), 1.74 (s, 15H), 3.49 (s, 6H), 4.40 (s, 2H); **13**: 1.28 (s, 18H), 1.47 (s, 36H), 4.05 (s, 6H), 4.49 (s, 4H); ratio **11**:**13** = 6:1.

Crossover exchange experiment between 1 and 3, and azulene: Compounds **1** and **3** (0.6 mmol) and azulene (1.2 mmol) were dissolved in ether (20 mL). After stirring for 12 hours at room temperature all volatiles were pumped off and the solid purple-black residue was dissolved in ether/acetonitrile (1:1), filtered, concentrated, and cooled to −30 °C for 24 hours giving black microcrystalline material (430 mg) representing a mixture of **7**, **8** and **20a,b** in a 2:13:1 ratio according to ^{1}H NMR analysis. Aside from the signals for **7** and **8**, resonances for the Me$_5$Cp and *tert*-butyl-Cp groups of **20a,b** were observed at $\delta = 1.56$ (Me$_5$Cp), 1.55 (Me$_5$Cp), 1.47 (*tert*-butyl), and 1.42 (*tert*-butyl). Other resonances of **20a,b** are obscured by signals of the major component **8**. MS of the mixture of **7**, **8**, and **20a,b** (fractional sublimation technique): EI (70 eV, $T_{vap} = 110$ °C): *m/z* (%): **20a,b**: 614(100) [M^+], 420 (6), 322 (22), 128(4). Aside from **20a,b** the homo Cp^R complexes **7** and **8** were observed at T_{vap} 150 °C and 160 °C, respectively, and gave identical spectra as observed for the pure samples.

X-ray structural analysis: Compound **3**: $C_{41}H_{66}Co_2$, $M_r = 676.8$, crystal size $0.35 \times 0.35 \times 0.35$ mm, monoclinic, $P2_1/c$ (No. 14), $a = 16.310(4)$ Å, $b = 11.909(2)$ Å, $c = 19.820(4)$ Å, $\beta = 98.97(1)°$, $V = 3802.4(1)$ Å^3, $\rho_{calcd} = 1.18$ g cm^{-3}, $\mu = 8.95$ cm^{-1}, $F(000) = 1464$ e, $Z = 4$, $\lambda = 0.71069$ Å, ω-2θ scan, 9421 measured reflections $(+h, +k, +l)$, $[(\sin\theta)/\lambda]_{max}$ 0.65 Å^{-1}, 8653 independent with 4446 observed reflections $[I > 2\sigma(I)]$, 388 refined parameters; the structure was determined by heavy atom methods, H positions were calculated and refined in fixed positions, $R = 0.073$, $R_w = 0.072$ $[w = 1/\sigma^2(F_o)]$, $R_{av} = 0.01$, max. residual electron density 0.58 e Å^{-3}.

Compound **8**: $C_{44}H_{66}Co_2$, $M_r = 712.9$, crystal size $0.14 \times 0.53 \times 0.53$ mm, triclinic $P\bar{1}$ (No. 2), $a = 9.470(1)$ Å, $b = 13.300(1)$ Å, $c = 16.357(2)$ Å, $\alpha = 96.13(1)°$, $\beta = 91.78(1)°$,$\gamma = 103.01(1)°$, $V = 1992.4(2)$ Å^3, $\rho_{calcd} = 1.19$ g cm^{-3}, $\mu = 8.57$ cm^{-1}, $F(000) = 768$ e, $Z = 2$, $\lambda = 0.71069$ Å, ω-2θ scan, 9391 measured reflections $(+h, +k, +l)$, $[(\sin\theta)/\lambda]_{max}$ 0.65 Å^{-1}, 9072 in dependent with 5966 observed reflections $[I > 2\sigma(I)]$, 415 refined parameters; the structure was determined by heavy atom methods, H positions were calculated and refined in fixed positions, $R = 0.062$, $R_w = 0.056$ $[w = 1/\sigma^2(F_o)]$, $R_{av} = 0.01$, max. residual electron density 0.65 e Å^{-3}.

Compound **9**: $C_{47}H_{72}Co_2$, $M_r = 754.91$, crystal size: $0.21 \times 0.42 \times 0.70$ mm, monoclinic, $P2_1/a$ (No. 14), $a = 13.262(2)$ Å, $b = 19.688(3)$ Å, $c = 16.831(3)$ Å, $\beta = 107.536(11)°$, $V = 4190.4(10)$ Å^3, $T = 293$ K, $\rho_{calcd} = 1.197$ g cm^{-3}, $\mu = 0.821$ mm^{-1}, $F(000) = 1632$ e, $Z = 4$, $\lambda = 0.71069$ Å, 9067 measured reflections $[+h, +k, +l]$, $[\sin\theta/\lambda]_{max} = 0.65$ Å^{-1}, 8503 independent and 4612 observed reflections$[I > 2\sigma(I)]$, 442 refined parameters, H atoms were calculated and not refined in the final refinement by least squares, $R = 0.0539$, $R_w = 0.1285$ $[w = 1/\sigma^2(F_o^2) + (0.063P)^2 + 0.000P)$ with $P = (F_o^2 + 2F_c^2)/3]$, residual electron density 0.561 e Å^{-3}.

Compound **10**: $C_{49}H_{76}Co_2$, $M_r = 782.96$, crystal size: $0.21 \times 0.32 \times 0.42$ mm, triclinic, $P\bar{1}$ (No. 2), $a = 11.399(3)$ Å, $b = 12.373(3)$ Å, $c = 16.199(2)$ Å, $\alpha = 95.034(15)$, $\beta = 91.17(2)°$, $\gamma = 106.86(2)$, $V = 2175.6(8)$ Å^3, $T = 100$ K, $\rho_{calcd} = 1.195$ g cm^{-3}, $\mu = 0.793$ mm^{-1}, $F(000) = 848$ e, $Z = 2$, $\lambda = 0.71069$ Å, 10255 measured reflections $[+h, +k, +l]$, $[\sin\theta/\lambda]_{max} = 0.65$ Å^{-1}, 9902 independent and 7501 observed reflections$[I > 2\sigma(I)]$, 764 refined parameters, H atoms were found and refined in the final refinement by least squares, $R = 0.0478$, $R_w = 0.1636$ $[w = 1/\sigma^2(F_o^2) + (0.1.000P)^2 + 0.000P)$ with $P = (F_o^2 + 2F_c^2)/3]$, residual electron density 0.799 e Å^{-3}.

Structures **8**–**10** are measured on a Enraf-Nonius-CAD4-diffractometer. Computing programs used in the structure calculations: EXPRESS/CAD4 (Enraf-Nonius), DATAP (Coppens, 1965), SHELXS-86 (Sheldrick, 1986), SHELXL-93 (Sheldrick, 1993), GFMLX (highly modified version of ORFLS; Busing, Martin & Levy, 1962), ORTEP (Johnson, 1976). Crystallographic data (excluding structure factors) for the structures reported in this paper have been deposited with the Cambridge Crystallographic Data Centre as supplementary publication no. CCDC-100568 and CCDC-101464. Copies of the data can be obtained free of charge on application to CCDC, 12 Union Road, Cambridge CB2 1EZ, UK (fax: (+44) 1223-336-033; e-mail: deposit@ccdc.cam.ac.uk).

ZINDO/S and MM+ force field computational procedure: These calculations were performed with the HyperChem computational package [Version 5.0, Hypercube, Waterloo, Ontario (Canada)]. Geometry optimizations (based on **1** and **3**) were carried out on the model complex [{(η^5-Cp)Co}$_2$-μ-{η^4:η^4-C$_6$H$_6$}] **4** with the ZINDO/1 method. For the ZINDO/1 geometry optimization the two long Co–C contacts each were fixed at

0947-6539/98/0410-1990 $ 17.50+.50/0 *Chem. Eur. J.* **1998**, *4*, No. 10

2.62 Å. Single-point LCAO-MO-SCF calculations with the ZINDO/S approximation with spectroscopic parametrization[15] were performed on the model complex **4** in its respective ZINDO/1 optimized geometry.

Acknowledgments: J.J.S. gratefully acknowledges funding of this research through the Fonds der Chemischen Industrie, the DFG (grant SCHN 375/6-1 and 6-2), and through a Heisenberg fellowship administered by the DFG. The work of C.J. is supported by the Fonds der Chemischen Industrie and the DFG. We thank Dr. D. Stöckigt and Dr. R. Mynott (MPI für Kohlenforschung) and their co-workers for recording MS and NMR spectra.

Received: October 30, 1998
Revised version: February 4, 1998 [F871]

[1] a) M. F. Semmelhack, *COMC II*, (Eds.: E. W. Abel, F. G. A. Stone, G. Wilkinson), Pergamon, **1995**, chapters 9.1 and 9.2, pp. 979–1070; b) T. G. Traylor, K. J. Stewart, *Organometallics* **1984**, *3*, 325; c) E. L. Muetterties, J. R. Bleeke, E. J. Wucherer, T. A. Albright, *Chem. Rev.* **1982**, *82*, 499; d) C. R. Landis, J. Halpern, *Organometallics* **1983**, *2*, 840; f) S. P. Nolan, R. L. de la Vega, C. D. Hoff, *Organometallics* **1986**, *5*, 2529.

[2] a) T. G. Traylor, K. J. Stewart, M. J. Goldberg, *J. Am. Chem. Soc.* **1984**, *106*, 4445; b) T. G. Traylor, M. J. Goldberg, *Organometallics* ***1987***, *6*, 2413; c) T. G. Traylor, K. J. Stewart, *J. Am. Chem. Soc.* **1986**, *108*, 6977; d) T. P. Gill, K. R. Mann, *Inorg. Chem.* **1980**, *19*, 3007; e) A. M. McNair, J. C. Schrenk, K. R. Mann, *Inorg. Chem.* **1984**, *23*, 2633; f) K. R. Mann, D. A. Freedman, D. J. Magneson, *Inorg. Chem.* **1995**, *34*, 2617; g) R. M. Nielson, M. J. Weaver, *Organometallics* **1989**, *8*, 1639; h) J. W. Kang, R. F. Chields, P. M. Maitlis, *J. Am. Chem. Soc.* **1970**, *92*, 720; i) A. Borbati, F. Calderazzo, R. Poli, P. F. Zanozzi, *J. Chem. Soc. Dalton Trans.* **1986**, 2569; j) R. G. Finke, R. H. Voegeli, E. D. Laganis, V. Boekelheide, *Organometallics* **1983**, *2*, 347; k) W. J. Boyer, J. W. Merkert, W. E. Geiger, A. L. Rheingold, *Organometallics* **1989**, *8*, 191; l) V. S. Leong, N. J. Cooper, *J. Am. Chem. Soc.* **1988**, *110*, 2644; m) D. R. Tyler, *Prog. Inorg. Chem.* **1988**, *36*, 125; n) S. B. Choe, J. J. Schneider, K. J. Klabunde, L. J. Radonovich, T. A. Ballantine, *J. Organomet. Chem.* **1989**, *376*, 419; o) S. B. Choe, K. J. Klabunde, *J. Organomet. Chem.* **1989**, *359*, 409.

[3] a) A. W. Duff, K. Jonas, R. Goddard, H. J. Kraus, C. Krüger, *J. Am. Chem. Soc.* **1983**, *105*, 5479; b) K. Jonas, *J. Organomet. Chem.* **1990**, *400*, 165; c) K. Cibura, Dissertation, Ruhr-Universität-Bochum, **1985**; d) W. Lammana, *J. Am. Chem. Soc.* **1986**, *108*, 2069; e) W. Lammana, W. B. Gleason, D. Britton, *Organometallics* **1987**, *6*, 1583; f) W. D. Harman, H. Taube, *J. Am. Chem. Soc.* **1987**, *109*, 1883; g) W. D. Harmann, M. Gebhard, R. Taube, *Inorg. Chem.* **1990**, *29*, 567; h) W. D. Harmann, H. Taube, *J. Am. Chem. Soc.* **1988**, *110*, 7555; i) F. A. Cotton, P. A. Kibala, W. A. Wojtcak, *J. Am. Chem. Soc.* **1991**, *113*, 1462; j) F. G. N. Cloke, K. A. E. Courtney, A. A. Sameh, A. C. Swain, *Polyhedron*, **1989**, *8*, 1641.

[4] J. J. Schneider, U. Denninger, O. Heinemann, C. Krüger, *Angew. Chem.* **1995**, *107*, 631; *Angew. Chem. Int. Ed. Engl.* **1995**, *34*, 592.

[5] a) J. J. Schneider, *Z. Naturforsch. B* **1995**, *50*, 1055; b) J. J. Schneider, habilitation thesis, University-GH Essen, **1993**.

[6] J. J. Schneider, U. Specht, *Z. Naturforsch. B* **1995**, *50*, 684.

[7] a) M. C. Zerner, G. H. Loew, R. F. Kirchner, U. T. Mueller-Westerhoff, *J. Am. Chem. Soc.* **1980**, *102*, 589; b) A. D. Bacon, M. C. Zerner, *Theor. Chim. Acta* **1979**, *53*, 21; c) M. C. Zerner, *Reviews in Computational Chemistry II* (Eds.: K. B. Lipkowitz, D. B. Boyd) VCH, Weinheim, **1991**, p. 313.

[8] a) H. J. Tobler, A. Bauder, H. H. Günthard, *J. Mol. Spectrosc.* **1965**, *18*, 239; b) G. W. Wheland, D. E. Mann, *J. Chem. Phys.* **1949**, *17*, 264.

[9] A. W. Hanson, *Acta Crystallogr.* **1965**, *19*, 19.

[10] C. H. Langford, H. B. Gray, *Ligand Substitution Processes*, Benjamin, New York, **1966**.

[11] a) M. L. Tobe, *Substitution reactions in Comprehensive Coordination Chemistry*, (Eds.: G. Wilkinson, R. D. Gillard, J. A. McCleverty) Pergamon, Oxford **1987**, chapter 7.1; b) R. B. Jordan, *Reaction Mechanism in Inorganic and Organometallic Chemistry*, Oxford University Press, **1991**.

[12] R. van Eldik, T. Asana, W. J. Le Noble, *Chem. Rev.* **1989**, *89*, 549.

[13] K. Jonas, E. Deffense, D. Habermann, *Angew. Chem.* **1983**, *95*, 729; *Angew. Chem. Int. Ed. Engl.* **1983**, *22*, 716; *Angew. Chem. Suppl.* **1983**, 1005.

[14] J. J. Schneider, D. Wolf, *Z. Naturforsch. B* **1998**, in press.

[15] a) T. G. Traylor, M. J. Goldberg, *J. Am. Chem. Soc.* **1987**, *109*, 396; b) A. Ceccon, A. Gambaro, F. Gottardo, S. Santi, *J. Organomet. Chem.* **1991**, *412*, 85; c) A. Ceccon, A. Gambaro, F. Gottardi, S. Santi, A. Venzo, *J. Organomet. Chem.* **1989**, *379*, 67; d) J. M. Buchanan, J. M. Stryker, R. G. Bergman, *J. Am. Chem. Soc.* **1986**, *108*, 1537.

[16] A. H. Janowicz, H. E. Bryndza, R. G. Bergman, *J. Am. Chem. Soc.* **1981**, *103*, 1516.